Multi-criteria analysis of the mechanism of degradation of Portland cement based mortars exposed to external sulphate attack

Rana El-Hachem, Emmanuel Rozière, Frederic Grondin, Ahmed Loukili

Multi-criteria analysis of the mechanism of degradation of Portland cement based mortars exposed to external sulphate attack

R. El-Hachem, E. Rozière, F. Grondin, A. Loukili

LUNAM Université, Institut de Recherche en Génie Civil et Mécanique (GeM), UMR-CNRS 6183, Ecole Centrale de Nantes, France

This work aims to contribute to the design of durable concrete structures exposed to external sulphate attacks (ESA). Following a preliminary study aimed at designing a representative test, the present paper suggests a study on the effect of the water-to-cement (w/c) ratio and the cement composition in order to understand the degradation mechanisms. Length and mass measurements were registered continuously, leached calcium and hydroxide ions were also quantified. In parallel, scanning electron microscopy observations as well as X-ray microtomography were realised at different times to identify the formed products and the crack mor-phology. Test results provide information on the basic aspects of the degradation mechanism, such as the main role of leaching and diffusion in the sulphate attack process. The mortar composition with a low w/c ratio leads to a better resistance to sulphate attack because the microstructure is less permeable. Reducing the C_3A content results in a macro-cracking decrease but it does not prevent expansion, which suggests the contribution of other expansive products, such as gypsum, in damage due to ESA. The observation of the cracks network in the microstructure helps to understand the micro-mechanisms of the degradation process.

1. Introduction

One of the most important issues in the design of concrete structures is their durability and maintenance. In aqueous media, cementitious materials are subjected to external chemical attacks; for instance constructions in contact with sea water, sewages, tunnels and also deep foundations in contact with groundwater [1]. Some case studies may be cited. St John [2] examined thin sections of concrete taken from the concrete linings of rail tunnels and revealed the presence of exfoliated layer (cracks filled with gypsum) due to a contamination with sodium sulphate. Diamond and Lee [3] examined also samples of concrete exposed for many years to sulphate-bearing soils and they observed a degradation zone of the slabs in contact with the soil. In the study of Leemann and Loser [4], a 45 year old concrete in a vertical ventilation shaft exposed to ground water containing sulphate was examined. Concrete was damaged and severe spalling was detected due mainly to ettringite formation.

Sulphate ions from surrounding water penetrate by diffusion and/or absorption in the concrete porous network and react with existing hydration products. In the presence of calcium hydroxide and water, monosulphate reacts with sulphate to produce ettringite [5–7]. Gypsum, in addition to ettringite can be produced during sulphate attack especially at low pH or if the surrounding solution contains a high concentration of sulphates. The stability of ettringite is a pH dependant as reported in literature [8–10]. Ettringite is known to be unstable below a pH around 10.5 and dissolves as gypsum and aluminium sulphate [10]. The formation of these products may cause expansion, cracking, spalling, softening, loss of strength and other forms of damage. Physical and chemical factors can influence the external sulphate attack [11], such as the properties of the solution (pH, concentration, the associated cation (sodium, calcium, magnesium)), the material properties (the type of cement, the water-to-cement (w/c) ratio) or the curing conditions.

A maximum w/c ratio is recommended by many committees (ACI, CEMBUREAU, CEN) beside the cement composition for given exposure conditions. The w/c ratio is actually one of the main factors that control the durability of concrete. A low w/c ratio induces a relatively high strength and low permeability but these effects do not systematically result in good resistance to sulphate attack. Some researchers actually found that cement pastes and concrete mixtures with a low w/c ratio showed a better resistance to sulphates [12–14] because the permeability was greatly reduced and penetration of sulphate solution into concrete was significantly lowered. Conversely, much higher w/c-ratios resulted in more rapid ingress of sulphate ions into the concrete. Other researchers [15,16] showed that the reduction of the w/c ratio in blended cement increased the expansion of mortar specimens and that a dense mixture was highly damaged especially in magnesium sulphate environment. Lower deterioration of some blended cements exposed to the sodium sulphate environment is attributed to the reduced calcium hydroxide content, which significantly reduces the effect of the sulphate attack in these cements. Therefore, there is a need to conduct additional investigations on the mechanism by varying the w/c ratio, one of the most discriminate criteria in concrete design.

Several expansive products are involved in sulphate attacks. The most often cited are ettringite and gypsum. According to chemical reactions, their proportions depend on the cement composition. Thus requirements on so-called sulphate-resisting cements, limiting the maximum C_3A contents, are often defined in standards (AASHTO M85, ASTM C 150, EN 206-1) in order to prevent ettringite formation. Previous works have also shown the gypsum damage potential for low C_3A cements [17,18]. But the parameters through which the formation of expansive products leads to damage in cementitious materials are still not well understood. As experimental studies mainly deal with global indicators such as expansion and boundary conditions may not be controlled and they are not being representative for exposure conditions in terms of sulphate concentration (ASTM C 1012). It is generally not possible to identify the causes of damage. Therefore experimental studies must be designed in a way to provide information at the macroscopic and microscopic levels. With this approach, it should be possible to assess to what extent the expansive products are involved in the degradation mechanism.

An experimental procedure has been defined on the basis of previous studies on the effect of the specimen size and the sulphate solution concentration [19,20]. The boundary conditions (temperature, pH, sulphate concentration) were well controlled. These studies showed that it is possible to choose the specimen size and the sulphate concentration to design a procedure showing an acceptable response time while maintaining the representativeness of the test [21]. The $2\times2\times16$ cm^3 mortar specimens were selected because of the consistency between the aggregate sizes and the specimen dimensions.

This article presents a multi-criteria study on the behaviour of mortars exposed to external sulphate attack providing contribution to understand the degradation kinetics due to external sulphate attacks. A test programme has been designed in order to evaluate the influence of w/c and cement composition on the extent and kinetics of degradation. Observations were made on different cement mortars exposed to a sodium sulphate concentration at 3 g/L of sulphates. The 3 g/L SO_4^{2-} concentration can be found in seawater [22,23]. Referring to the European standards, this concentration is below the limits of the XA3 exposure class for surface and ground waters (EN 206-1). This study includes macroscopic and microscopic measurements. Mass and length measurements were registered every time the solution was renewed. In addition, the leaching kinetics were assessed. Microstructural alterations were investigated by a scanning electron microscope and an X-ray microtomograph.

2. Material and mixture characteristics

Two cements were tested in this study. The main differences between these two cements are the C_3A and C_4AF contents:

Table 1
Cements properties.

	Ordinary Portland cement (OPC)	Sulphate resisting cement (SRC)
Chemical analysis (%)		
CaO	65.4	65.9
SiO_2	20.4	21.3
Al_2O_3	4.9	3.7
Fe_2O_3	1.8	4.5
SO_3	3.6	2.6
Compound composition of clinker (%)		
C_3S	66.4	67.5
C_2S	5.6	6.7
C_3A	11.4	2.2
C_4AF	5.4	13.8
Physical properties		
Blaine fineness (cm^2/gr)	3750	3460
Normal comp. strength (MPa)	69.1	64

Table 2
Mortar compositions.

	M1	M2	M3
Siliceous sand (kg/m^3)			
0/2	1409	1409	1409
Cement (C) (kg/m^3)			
OPC	495	596	
SRC			602
Water	301	268	266
w/c	0.6	0.45	0.45
Volume of paste Vp (L/m^3)	460	460	460

- OPC: Ordinary Portland Cement (C_3A content: 11.4%; C_4AF: 5.4%),
- SRC: Sulphate Resisting Cement (low C_3A content: 2.2%; C_4AF: 13.8%).

The cement composition is given in Table 1.

In order to avoid thaumasite formation due to calcium carbonate present in limestone aggregates [24,25], mortar mixtures have been designed with a siliceous sand.

The mortars M1 and M2 were made with the OPC at two different w/c ratios, respectively 0.60 and 0.45 (Table 2). Mortar M3 was derived from M2 by replacing the OPC by the SRC. The paste volume was maintained constant for all compositions. The lower w/c was chosen to comply with the requirements from the European standard (NF EN 206-1) for chemically aggressive environments.

3. Experimental procedure

3.1. Specimen preparation

Mortar specimens were cast as $2\times2\times16$ cm^3 prisms. They were cured at 100% relative humidity (RH) for 24 h. Then they were demoulded and stored in limewater for two different periods, 3 and 28 days, until immersion in a sodium sulphate solution (3 g/L of SO_4^{2-}) prepared with demineralised water. In parallel, identical specimens were stored in tap water. The prisms had gauge studs at both ends in order to measure expansion with length comparators. In addition, a resin layer was applied at these ends and also coated at 5 mm on the other sides to prevent the sulphate solution from penetrating at the ends. If the ends of the specimens were not coated, the measured expansion would be more affected by the ends than the mid-length portions of the bar. This protection helps to get more representative and reproducible results for the length change [26,27].

3.2. Sulphate ageing test

The device used for the sulphate test is presented in Fig. 1 [28].

Tests have been realised in controlled conditions at a constant pH of 7.5. The pH was regulated by adding a nitric acid solution of 0.50 mol/l. The liquid/solid volume ratio of the batches was 14 to 1. The solutions were renewed every 15 ml of added acid to maintain the concentration gradients as a constant and to avoid the interference between nitrate and cement hydrates. The pH value is meant to be representative of field conditions in which concrete is exposed to continuous supply of sulphate ions [29–31]. If the pH was not controlled, it would raise to 12 or above after a short immersion period of the samples.

3.3. Microtomography

Samples were observed by microtomography using an XRadia MicroXCT-400 system. The energy used was 110 kVp X-rays. Successive rotations of the sample, 2000 projections, corresponding to 2000 angular positions ranging between 0° and 360°, were acquired by a 4 megapixel (2048×2048) CCD-digital camera and an objective

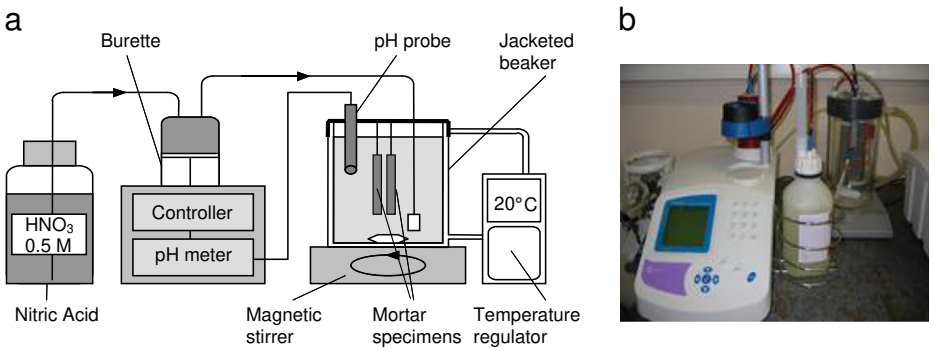

Fig. 1. Schematic diagram (a) and device (b) used for sulphate test.

revolver, that can be used to choose the desired magnification. Filters were used to compensate for beam hardening. The pixel size was 28 μm and the exposure time was 4 s for each image. The data scanned with the Xradia device is reconstructed with Xradia's own software.

3.4. Scanning electron microscopy

SEM investigation was used to analyse the microstructure of the specimens attacked by sulphates. The SEM is equipped with an EDX-detector that allows EDX analysis including mapping. The specimens used for SEM observations were 3 cm thick slices from the $2\times2\times16$ cm^3 mortar prisms. After 7 days of drying at 20 °C and 50% RH, the specimens were embedded in a low-modulus epoxy and were polished using progressively finer grids. The pressure in the specimen chamber was 50 Pa and the accelerating voltage was 15 kV. The observations were performed by backscattered electrons imaging. The elemental mappings were obtained under a magnification of 650×, covering approximately a 140×190 μm area. The EDS point analysis on ettringite was carried out at relatively high magnification (>30000).

4. Chemo-mechanical analysis

4.1. Mechanical analysis

The relative longitudinal deformation (differences between the specimens stored in sulphate solution and control) is presented in Fig. 2. Two phases of evolution were identified on both curves regardless of composition and cement type. A latency period was observed corresponding to no significant macroscopic strain (identified in Fig. 2 with an arrow on the mortar M2 curve). Then, a non-linear length increase appeared due to swelling of damaged mortar specimens. As an example, comparison could be made for mortars exposed to sulphates at day 28. The expansion began after 106 days of exposure to the sulphate solution for the mortar M1 while the latency period was longer for the mortar M2 (165 days). The SRC that should be resistant to sulphate attack showed also a moderate and slow expansion after 298 days of exposure.

To explain these observations, relative mass variations are plotted against square root of time in Fig. 3. Thus, the effect of sulphate attack is separated from the phenomena of absorption and hydration. The latency period was associated with a linear loss of mass (negative slope) for the three mortars. This linear variation according to the square root of time reflects a diffusion phenomenon with a negative balance. During this first phase, the ion flow coming out of the samples overcame the incoming flow sulphates ions, which explains the loss of mass. The diffusion has an important role in the degradation process. The second phase on the mass curve corresponds to the expansion. In the case of M1 and M2 mortars, the increase in volume induced an increase in mass. Dealing with mortar M3, the loss of mass at the surface (leaching) prevailed over the macroscopic swelling which could explain this continuous loss of mass.

The age of the mortars at the time of immersion was not a major parameter in this test. However, the mortars M1 exposed to sulphates after 3 days of curing were the first to show expansion followed by mortars exposed to sulphate at day 28. The difference for mortar M2 concerning the time of immersion is not significant. The expansion of mortars M2 exposed at day 3 began just seven days earlier than those exposed at day 28. The difference can be explained by the degree of hydration. On the one hand, short curing actually leads to higher permeability. On the other hand, the microporosity of the cement paste is higher at early age thus expansive products are likely to form causing less damage than in denser microstructures.

The expansion of mortar M1 began after three months of exposure to the sulphate solution while M2 did not show any significant

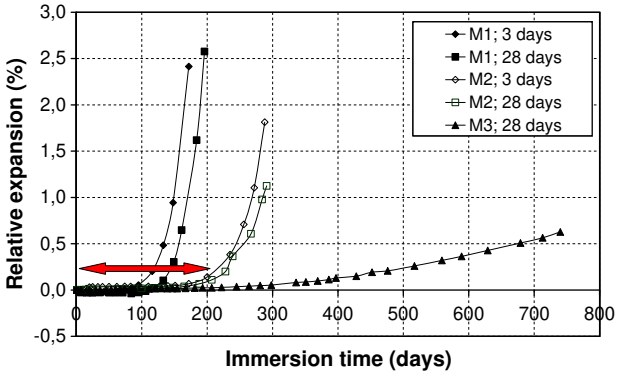

Fig. 2. Relative expansion of mortar specimens.

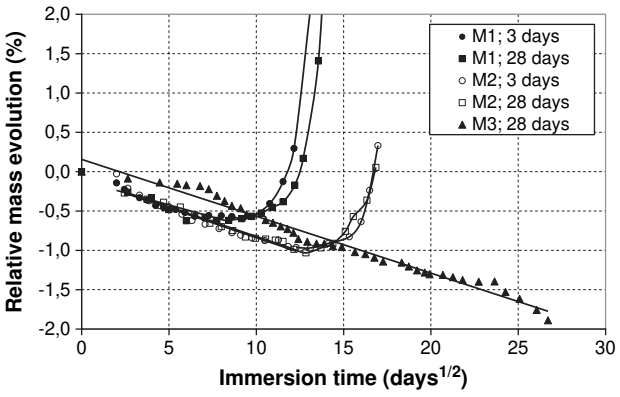

Fig. 3. Relative mass evolution of mortar specimens.

Table 3
Tensile and compressive strengths of mortars.

	M1	M2	M3
f_c 2 days (MPa)	21.5	35	36
f_c 28 days (MPa)	56	77.5	82
f_t 28 days (MPa)	7.9	10.1	10.2

expansion before six months. The mortar M3 was the last to show expansion after 8 months approximately. The slope of the expansion curves decreased respectively by reducing the w/c ratio and using a sulphate resisting cement. These results are consistent with the standards that prescribe the use of a sulphate resisting cement and limit the maximum w/c in an aggressive environment to 0.50 for the XA2 and 0.45 for the XA3 exposure classes (NF EN 206-1).

Several material properties could explain this difference, namely: the strength, the elastic modulus, and the diffusion coefficient.

4.2. Interpretation of results by the material properties

Table 3 gives the tensile (f_t) and compressive (f_c) strengths of the three different mortars. The M2 and M3 mortars showed the highest compressive strength, which is consistent with their low w/c.

The diffusion coefficient of sulphates ($D_{eff(mig)}$) was assessed through a steady-state migration test [32] on two different migration cells (Fig. 4) and calculated following this relation:

$$D_{eff(mig)} = \frac{R\,T\,L}{F\,U\,C_{upstream}} J_{downstream} \qquad \left[m^2.s^{-1}\right] \tag{1}$$

where R represents the ideal gas constant ($R = 8.314\ J.K^{-1}.mol^{-1}$), T is the temperature (K), L is the thickness of the sample (m), J is the sulphate ion flow crossing the sample ($mol.m^{-2}.s^{-1}$), F is the Faraday constant ($F = 96480\ C.mol^{-1}$), U is the tension (V) and $C_{upstream}$ is the sulphate ion concentration in the upstream compartment ($mol.l^{-1}$).

The mean diffusion coefficient measured on mortar M1 was equal to $1.84\times10^{-12}\ m^2\ s^{-1}$ and is almost double of the mortar M2 coefficient that was equal to $1.06\times10^{-12}\ m^2\ s^{-1}$. This is related to the dense structure of the mortar with low water content.

When the w/c ratio is high, the system is more permeable, thus less resistant to sulphate attack. This result depends also on the pore size distribution.

As shown in Fig. 5, for all compositions, the initial porosity for the control specimens decreased with time due to the hydration of the cement. The w/c-ratio controls the total porosity. A high ratio generates a more porous cement matrix. The M2 and M3 mortars had a lower porosity than M1, due to the different amount of cement and water in both compositions. Dealing with the evolution of the porosity during the attack, no change could be shown between the initial

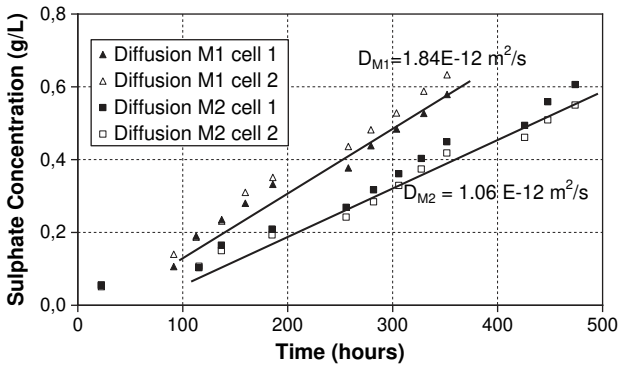

Fig. 4. Sulphate diffusion for the two different mortars.

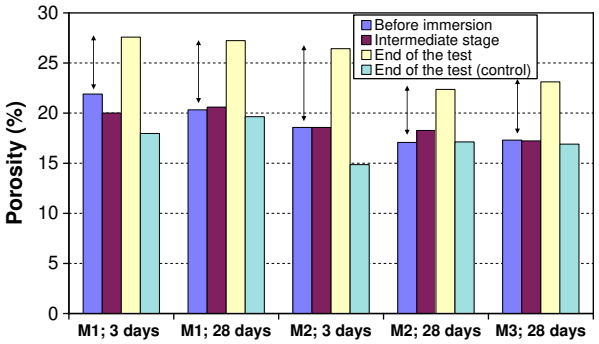

Fig. 5. Bulk porosity evolution of the three different mortars.

and the intermediate stage while at the final stage the increase was significant. This increase in porosity at the final stage can be attributed to the presence of microcracks and macrocracks. For example, the porosity of the sample M1 exposed at 28 days increased from 20.6% to 27.2% between the initial and final stage. The higher initial porosity of the 3 days immersed samples in comparison to the 28 days could be the possible reason why the mortars exposed at 3 days showed earlier expansion: sulphates could penetrate more easily into the specimens.

But how can the loss of mass be explained during the latency period shown in Fig. 2? Water surrounding the mortars caused leaching. This corresponds to the dissolution of portlandite, releasing calcium and hydroxide ions. During the latency period, the sulphate ions reacted with the products of cement hydration, such as portlandite and hydrated aluminates to form expansive products. The latency period would thus correspond to a phase of competition between leaching and the sulphate ion ingress and reaction with the hydration products resulting in a loss of mass and a porosity increase. Therefore, it is interesting to quantify the leached ions.

4.3. Definition of a degradation mechanism

As the three mortars were designed keeping the volume of paste constant, the initial calcium hydroxide content is higher in the M2 and M3 mortars. To eliminate this effect in order to explain the degradation mechanisms, the quantity of leached ions should be reported to the initial CaO content of the binder. Equivalent damaged depths (EDD) may be calculated [33]. This depth is defined as the ratio between the amount of leached calcium (mol/m^2) at a time 't' and the theoretical initial total calcium content in the binder (mol/m^3). From the solution titration, leached calcium can be calculated and the initial CaO of the cement content is given by the producers. The EDD is calculated by the following equation:

$$EDD_{(t)} = \frac{Leached\ \ calcium_{(t)}}{Initial\ \ calcium\ \ content\ \ in\ \ binder}. \tag{2}$$

EDD is plotted vs. the square root of time in Fig. 6. The M1 samples showed the greatest EDD at early ages as they had the highest diffusion coefficient. The same conclusions could be drawn for the samples exposed at 3 days compared to those exposed at 28 days. The M1 and M2 curves lost the linearity. This loss of linearity correlated with the beginning of the expansion (see Figs. 2 and 3). The increase in the leaching rate is actually due to the increase of diffusion as the material is damaged [34] by the expansion that exceeds the tensile strain capacity of mortar. The loss of linearity is not observed on M3 curve. Leaching increased at a constant rate, which would mean that the diffusion coefficient was not significantly affected by sulphate attack. The leached zone reached at the end of the test is thicker for the M3 specimens than for M2 and M1.

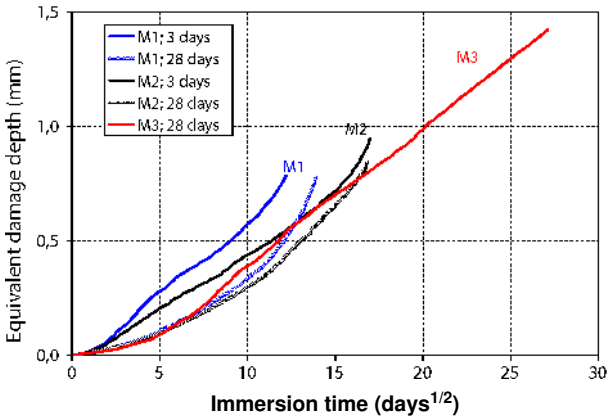

Fig. 6. Leaching. EDD vs. square root of immersion time.

The ettringite front ingresses faster than the leaching front [7]. The ingress of the ettringite front is difficult to assess continuously, thus the leached portlandite front was used as an indicator of the sulphate ingress, as diffusion is involved is both cases. In Fig. 7 the expansion of the specimens is plotted against leached calcium hydroxide. For a given type of cement, a common threshold of leaching was required to trigger the expansion of the mortar. This could not be showed for mortar M3 as the cement type was not the same. The initiation time of swelling would correspond to the same ingress of sulphate, which could be linked to a relative critical proportion of the cross section of the specimens required to generate global swelling (Fig. 8). As tensile stresses are generated in the central area, the tensile strength of mortars could be expected to be an important parameter. M2 mortar showed higher tensile strength than M1 mortar. The experimental results showed that the behaviour was actually more dependent on diffusion, but this result need to be confirmed by numerical analysis.

5. Microstructure analyses

To confirm the assumptions on the degradation mechanism derived from the macroscopic changes, observations and analysis of the microstructure were carried out, namely: scanning electron microscopy (SEM) observations, EDS analysis (Energy Dispersive X-Ray Spectroscopy) and microtomography.

5.1. Microtomography observations

The cross section (A) in specimens (Fig. 9) highlights the contrast between the degraded outer zone and the undamaged core. This confirms that the formation of expansive products in the external area in contact with the solution is responsible for the overall deformation.

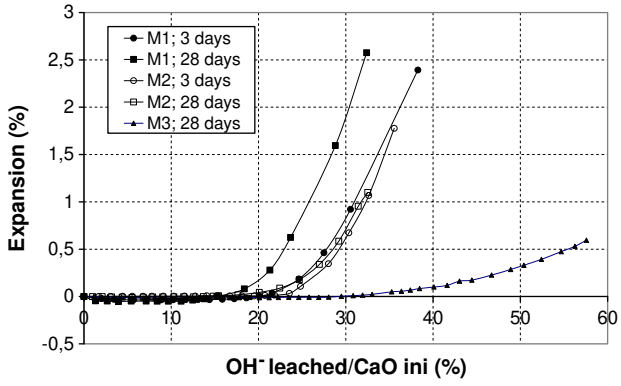

Fig. 7. Expansion vs. leached calcium hydroxides.

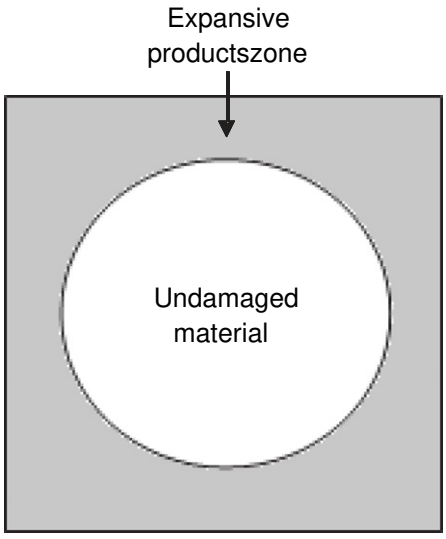

Fig. 8. Relative required critical section to generate swelling.

Moreover microtomography observations (Fig. 10) of the degraded samples showed the main cracks on several sections of the specimens. The increase of porosity due to leaching is well visible on mortar M3 because the pores are not filled with reaction products of the sulphate attacks as it is the case in mortars M1 and M2. Although the better resistance of the M2 samples against sulphate attacks in terms of expansion, it should be noted that those specimens were visibly more degraded than the M1 samples at the same macroscopic level of deformation. The denser structure of the M2 composition showed wider cracks.

These results are similar to those of Naik et al. [35] who observed a higher expansion for high w/c ratios and showed by tomography that the samples with a low w/c ratio were more affected by macro-cracking. The first physical manifestations of damage appeared earlier and the progress of the damage was also faster in the lower w/c samples. At the microscopic scale, the tensile strength was exceeded which could explain these transversal cracks observed on the longitudinal section (B).

The M3 samples showed clearly less macro-cracks than M1 and M2 samples, even if transversal cracks could be detected on the longitudinal section (Fig. 10). In spite of significant expansion, M3 specimens could have been less damaged. Less ettringite can form as the C_3A content of the cement is lower. This could also explain why the expansion rate of M3 specimens was lower (Fig. 2).

M3 specimens showed constant leaching rate (Fig. 6) whereas M1 and M2 specimens showed increasing diffusion with time. This is consistent with lower damage [34,36] and less ettringite formed. When observing SRC cubes stored in a Na_2SO_4 solution, Gollop and Taylor [37] showed also that in the outermost 50–100 μm, the paste had the dark appearance characteristic of decalcified material. At the cube edges, cracking was much less marked than with the OPC.

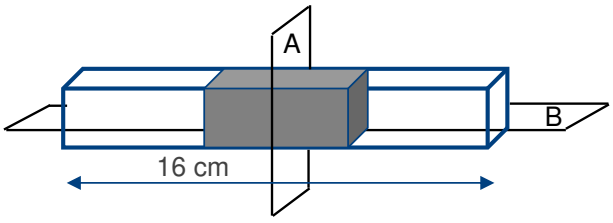

Fig. 9. Retained section for microtomography observations.

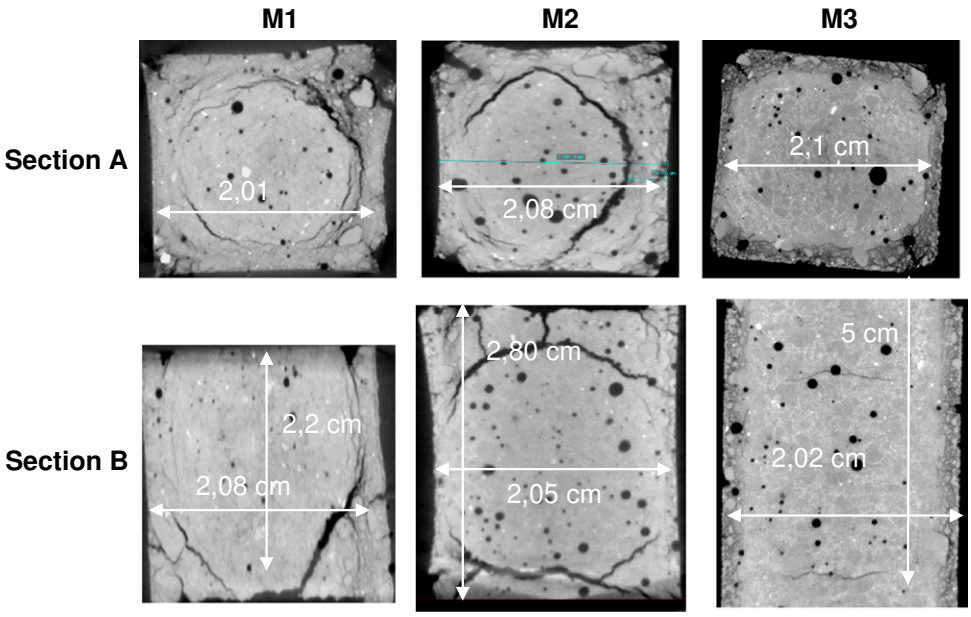

Fig. 10. Microtomography pictures for degraded samples; (M1. Top; M2. Middle; M3. Bottom).

5.2. SEM observations: gypsum and ettringite formation

Analyses of the microstructure were conducted in order to identify the products of the reactions between sulphate ions and cement hydration products. SEM observations were made on the three mortars for the samples with different immersion times (3 and 28 days) (Fig. 11). Analyses were done at the beginning of expansion (intermediate phase) (75 days for mortar 'M1; 3 days', 106 days for mortar 'M1; 28 days', 158 days for mortar 'M2; 3 days', 165 days for mortar 'M2; 28 days' and 298 days for mortar M3) and at the end of the test (degraded sample). The same conclusions could be drawn for mortar M1 and M2. At the intermediate stage, gypsum was present in the external zones (1.5 mm maximum from the borders of the specimens) while ettringite was formed deeper (from 1.5 to 2.5 mm). At the end of the tests, the external zone was totally leached, leading to a non cohesive paste. These results join those of

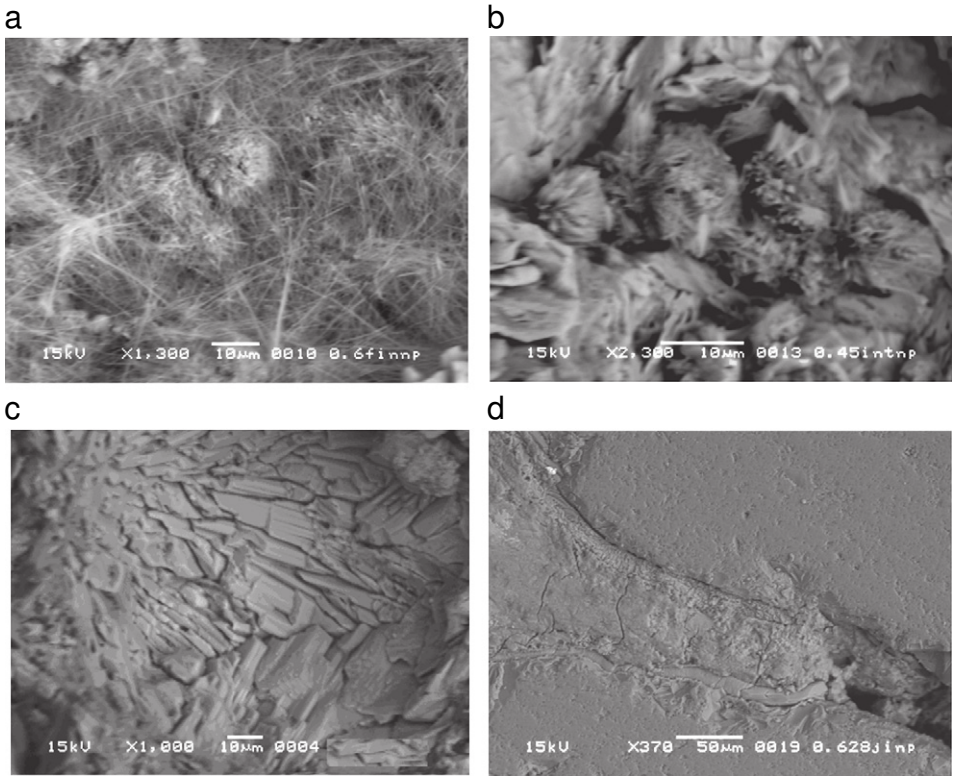

Fig. 11. PC mortar specimen (M1 and M2) stored in sodium sulphate solution, showing formation of (a) ettringite ('M1; 3 days' after 172 days of exposure), (b) coexistence of gypsum and ettringite ('M2; 28 days' after 165 days of exposure) and (c and d) gypsum ('M2; 3 days after 158 days of exposure and 'M1; 28 days' after 196 days of exposure) respectively.

Golllop and Taylor [38] reporting that C—S—H is markedly decalcified at the surface of PC paste after the complete dissolution of CH when it was exposed to Na_2SO_4 solution. A large crack was dividing the cross section of the sample into two parts (Fig. 10—Section A): one significantly damaged and another not damaged. Gypsum was formed until 3.5 mm from the borders. Ettringite was found deeper from 1.5 to 4 mm. For the mortar M3, gypsum was the mainly observed product formed and no ettringite was detected, which is consistent with the low C_3A content of this cement. The SRC was also richer in C_4AF, but the influence of this parameter is still not well understood. The influence the C_3A content of the OPC is actually consistent with the formation of ettringite from monosulphate.

The presence of gypsum and ettringite detected morphologically by SEM observations was then confirmed by Energy Dispersive Spectroscopy (EDS) analysis. Fig. 12 shows an EDS analysis on an attacked mortar sample (exposed at 28 days). The results consist in maps of calcium, silica, sulphur, and aluminium relative concentrations. The high calcium concentrations corresponded to the cement paste and the highest silica concentrations referred to the aggregates as siliceous sand was used. Relatively high sulphur concentrations could be observed around aggregates. They were associated with high calcium concentrations. This reveals the presence of gypsum ($CaSO_4$, $2H_2O$) formed referring the following equation:

$$Ca(OH)_2 + SO_4^{2-} + 2H_3O^+ \rightarrow CaSO_4.2H_2O + 2H_2O. \quad (3)$$

Ettringite ($C_3A.3C\overline{S}.H_{32}$) was also present and confirmed by EDS analysis for the M1 and M2 compositions: a high localised

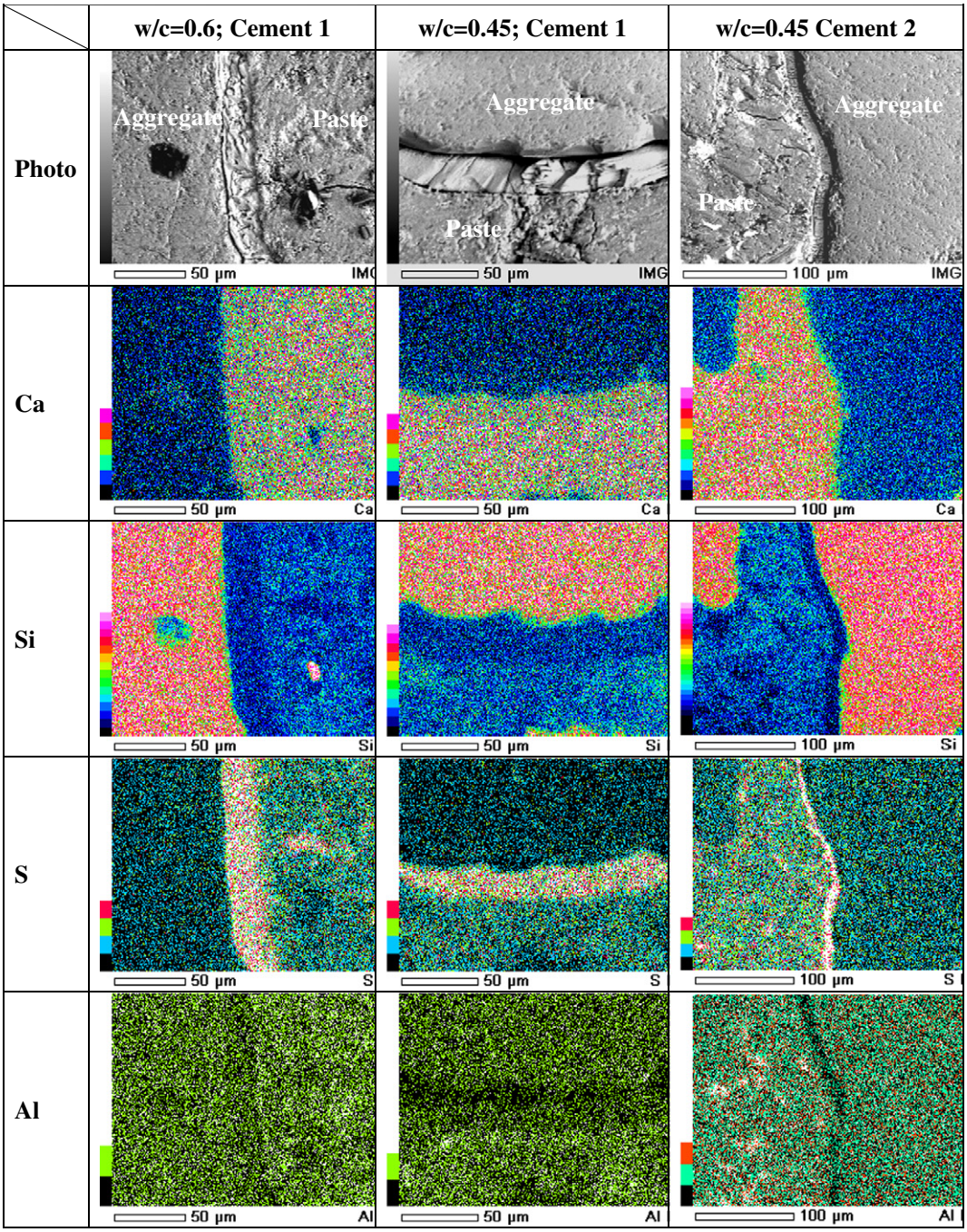

Fig. 12. Energy dispersive spectroscopy (gypsum veins filling the ITZ).

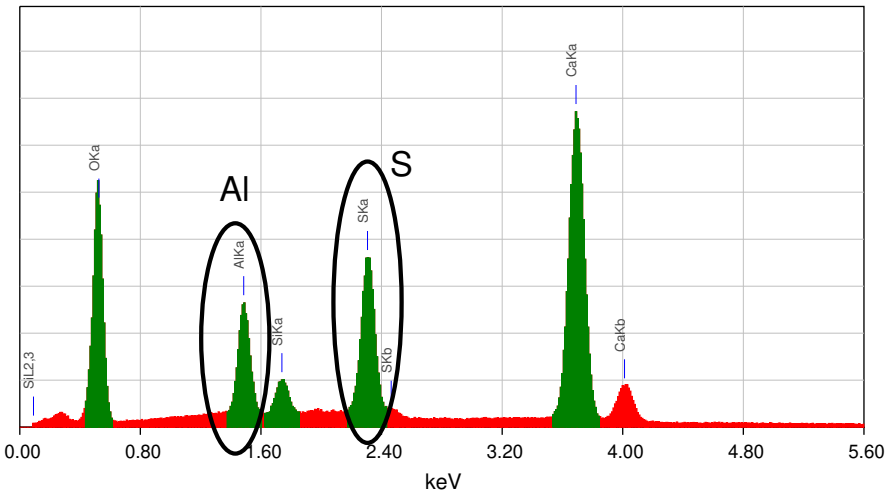

Fig. 13. Spectrum from EDS area analysis on photo A of Fig. 11 (M1; 3 days).

concentration of aluminium and sulphur was detected. Fig. 13 shows the spectrum of EDS analysis on an area analysis of Fig. 11-a. The atomic proportions were also quantified and the results are summarised in Table 4.

Gypsum crystals were mainly formed in the interfacial transition zone (ITZ) and in the cracks while ettringite was found in the pores of the cement paste. The formation of these products could be associated with swelling, cracking and spalling. However, it is not clear if the gypsum or ettringite formation is the cause or the consequence of swelling. It depends on whether these products are located in pre-existing voids or cracks, or whether the cracks were the consequence of expansion by ettringite or gypsum formation. Mehta [39] explained the presence of gypsum in the ITZ by microcracks existing previously to sulphate exposure. These microcracks, larger than capillary pores, are a preferential path for the creation of interconnections leading to a more permeable system. So the sulphate ion diffusion is easier in this zone. Bonen and Sarkar [40] have also studied the replacement of CH by gypsum in the ITZ and they found thick deposits of gypsum up to 50 μm precipitating in this zone by a through-solution mechanism. These observations showed the important role of the ITZ that would be absent if the investigation was led on paste samples. Ettringite is not stable at low pH (below 11.5–12) [8]. That is why it could not be found in the external zone in contact with controlled pH solution. During the penetration of sulphate ions, ettringite was likely to be formed first, when pH of mortar had not dropped yet. Hence, it was found in deeper layers than the other products. Then the decrease in pH would have it transformed to gypsum, as pH was kept constant at 7.5 in the sulphate solution. Gollop and Taylor [38] explained this distribution of formed products as follows: ettringite crystallisation ends when the alumina provided by AFm phase became insufficient. Hence, sulphates react with Ca^{2+} to form gypsum. The portlandite is consequently decomposed. Further decalcification and leaching occur. Gypsum is usually detected in the outer layers beyond the maximum distribution of ettringite which is the case in our study.

Table 4
Quantitative analysis of the spectrum presented in Fig. 13.

Element	Normalised conc (wt %)	Error	Atomic proportion (%)
O	46.39	0.1	66.15
Al	5.35	0.04	4.52
Si	1.78	0.05	1.44
S	10.03	0.04	7.13
Ca	36.46	0.09	20.75
Total	100		100

The SEM observations at the beginning and at the end of expansion make it possible to illustrate an assumption on the spatial distribution of formed products during sulphate attack (Fig. 14). The internal zone of the attacked specimen can be associated to an undamaged or slightly affected material whereas the external zone corresponds to the formation of the expansive products.

6. Conclusion

This paper presents the results of a study that aimed to explain the degradation mechanism of mortars exposed to external sulphate attack (ESA) through variations of the composition. The composition parameters were the w/c ratio and the cement type. Three mortar mixtures M1, M2 and M3 cast as $2\times2\times16$ cm^3 prisms were exposed to a sodium sulphate solution with moderate sulphate concentration (3 g/L of SO_4^{2-}) and controlled pH. M1 and M2 were made with the same type of cement (OPC with a high C_3A content) but two different w/c ratios (0.60 and 0.45 respectively). A sulphate resistant cement (SRC with low C_3A content) was used for the M3 composition (w/c = 0.45). The test procedure was designed to keep the boundary conditions constant.

- The sulphate ion ingress has to reach a critical proportion of the cross section of the prisms to trigger the global expansion of the specimens. This was confirmed by microtomography which showed damaged external layer and unaltered core with transversal cracks. They were observed on the three series of specimens.
- Leaching is important for the degradation mechanism. The dissolution of portlandite $Ca(OH)_2$ goes together with external sulphate attack. It leads to increased porosity, easier sulphate ion diffusivity and formation of gypsum. Whatever the cement composition, the three mortars finally show expansion and cracking. The two

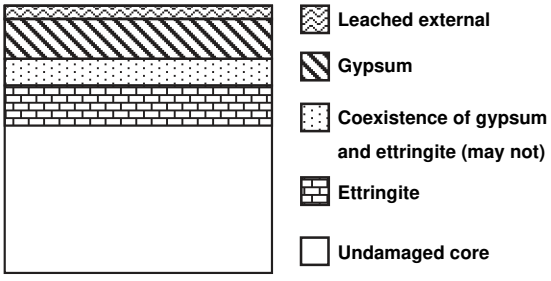

Fig. 14. Simplified scheme of expansive product formation.

cements had actually high CaO contents that increased their vulnerability to ESA.

- Varying the w/c ratio showed the influence of diffusion. The reduction in the w/c ratio resulted in a lower diffusion coefficient and delayed the measured expansion. However, once the initiation time of expansion was reached, the expansion rates were approximately the same and finally lead to continuous cracks, whatever the w/c ratio.
- The proportions of the expansive products and their potential of damage were shown to be affected by the C_3A-content. For given diffusion properties, the expansion due to sulphate ions depends on the chemical composition of the cement paste. The expansion rate increased when using cement with a high C_3A-content because of the influence of cracking on the diffusion properties of the damaged mortars. When low C_3A-content cement was used, macrocraking was moderate which resulted in constant expansion rate due to constant diffusion properties.

Acknowledgments

The authors would like to thanks Dr Christian Burtin from the GeM Institute for his useful help in realising the microtomography observations.

References

[1] J. Figg, Field studies on sulfate attack on concrete, In: J. Marchand, J.P. Skalny (Eds.), Materials Science of Concrete: Sulfate Attack Mechanisms, American Ceramic Society, Westerbrook, Ohio, 1999, pp. 315–323.
[2] D.A. St John, An unusual case of ground water sulfate attack on concrete, Cem. Concr. Res. 12 (1982) 633–639.
[3] S. Diamond, R.J. Lee, Microstructural alterations associated with sulfate attack in permeable concretes, In: J. Skalny, J. Marchand (Eds.), Material Science of Concrete - Sulfate Attack Mechanisms, American Ceramic Society, Westerville, OH, 1999, pp. 123–174.
[4] A. Leemann, R. Loser, Analysis of concrete in a vertical ventilation shaft exposed to sulfate-containing groundwater for 45 years, Cem. Concr. Compos. 33 (2011) 74–83.
[5] C.D. Laurence, Sulphate attack on concrete, Mag. Concr. Res. 42 (153) (Dec 1990) 249–264.
[6] P.K. Mehta, P. Schiessl, M. Raupach, Performance and durability of concrete systems, In: Proceedings, 9th International Congress of the chemistry of Cement, New Delhi, India, vol. I, 1992, pp. 571–659.
[7] B. Lothenbach, B. Bary, P. Le Bescop, T. Schmidt, N. Leterrier, Sulfate ingress in Portland cement, Cem. Concr. Res. 40 (2010) 1211–1225.
[8] M. Santhanam, M.D. Cohen, J. Olek, Sulfate attack research — whiter now? Cem. Concr. Res. 31 (2001) 845–851.
[9] D. Damidot, F.P. Glasser, Thermodynamic investigation of the CaO–Al2O3–CaSO4–H2O system at 25 °C and the influence of Na2O, Cem. Concr. Res. 23 (1) (1993) 221–238.
[10] A. Gabrisová, J. Havlica, S. Sahu, Stability of calcium sulphoaluminate hydrates in water solutions with various pH values, Cem. Concr. Res. 21 (6) (1991) 1023–1027.
[11] J. Prasad, D.K. Jain, A.K. Ahuja, Factors influencing the sulphate resistance of cement concrete and mortar, Asian J. Civ. Eng. 7 (3) (2006) 259–268.
[12] P.J.M. Monteiro, K.E. Kurtis, Time to failure for concrete exposed to severe sulfate attack, Cem. Concr. Res. 33 (2003) 987–993.
[13] P.K. Mehta, Concrete in the Marine Environment, Elsevier Applied Science, London and New York, 1991.
[14] J. Skalny, J. Marchand, I. Older, Sulfate Attack on Concrete, Spon Press, New York, 2002..
[15] G.L. Kalousek, L.C. Porter, E.J. Benton, Concrete for long-time service in sulphate environment, Cem. Concr. Res. 1 (2) (1972) 79–89.
[16] O.S.B. Al-Amoudi, M. Maslehuddin, M.M. Saadi, Effect of magnesium sulphate and sodium sulphate on the durability performance of plain and blended cements, ACI Mater. J. 1 (92) (1995) 15–24.
[17] S.U. Al-Dulaijan, M. Maslehuddin, M.M. Al-Zahrani, A.M. Sharif, M. Shameem, M. Ibrahim, Sulfate resistance of plain and blended cements exposed to varying concentrations of sodium sulfate, Cem. Concr. Compos. 25 (2003) 429–437.
[18] M. Santhanam, M.D. Cohen, J. Olek, Effects of gypsum formation on the performance of cement mortars during external sulphate attack, Cem. Concr. Res. 33 (2003) 325–332.
[19] E. Rozière, A. Loukili, R. El Hachem, F. Grondin, Durability of concrete exposed to leaching and external sulphate attack, Cem. Concr. Res. 39 (2009) 1188–1198.
[20] R. El-Hachem, E. Rozière, F. Grondin, A. Loukili, New procedure to investigate external sulphate attack on cementitious materials, Cem. Concr. Compos. 34 (3) (2012) 357–364.
[21] R. El Hachem, Etude multi-critères de la dégradation des matériaux cimentaires par l'attaque sulfatique externe, PhD Thesis at Ecole Centrale de Nantes, 2010.
[22] E.G. Swenson, 'CBD-136-F. Le béton en milieux sulfatés', Conseil national de recherches Canada, , Avril 1974..
[23] M. Radojevic, V.N. Bashkin, Practical Environmental Analysis, Royal Society of Chemistry, Cambridge, 1999..
[24] Harald Justnes, Thaumasite formed by sulphate attack on mortar with limestone filler, Cem. Concr. Compos. 25 (2003) 955–959.
[25] S. Lee, R. Hooton, H. Jung, D. Park, C. Choi, Effect of limestone filler on the deterioration of mortars and pastes exposed to sulphate solutions at ambient temperatures, Cem. Concr. Res. 38 (2008) 68–76.
[26] C. Ferraris, P. Stutzman, Sulphate Resistance of Concrete: a New Approach and Test, PCA R&D Serial No. 2485, , 2005..
[27] C. Ferraris, P. Stutzman, M. Peltz, J. Winpigler, Developing a more rapid test to assess sulphate resistance of hydraulic cements, J. Res. Nat. Inst. Stand. Technol. 110 (2005) 529–540.
[28] E. Rozière, A. Loukili, Performance-based assessment of concrete resistance to leaching, Cem. Concr. Compos. 33 (4) (2011) 451–456.
[29] Amercian Ground Water Trust, The American Well Owner, Number 3, , 2003..
[30] J. Skanly, J. Marchand, I. Older, Sulfate Attack on Concrete, Spon Press, London, 2002..
[31] P.K. Mehta, Sulfate attack on concrete: separating myths from reality, Concr. Int. 22 (8) (2000) 57–61.
[32] C. Andrade, Calculation of chloride diffusion coefficients in concrete from ionic migration measurements, Cem. Concr. Res. 23 (1993) 724–742.
[33] C. Badoz, P. Francisco, P. Rougeau, A Performance test to estimate durability of concrete products exposed to chemical attacks, In: Proceedings of the second International congress of FIB, June 5–8, 2006.
[34] B. Gerard, J. Marchand, Influence of cracking on the diffusion properties of cement-based materials. Part I: influence of continuous cracks on the steady-state regime, Cem. Concr. Res. 30 (1) (2000) 37–43.
[35] N.N. Naik, A.C. Jupe, S.R. Stock, A.P. Wilkinson, P.L. Lee, K.E. Kurtis, Sulfate attack monitored by microCT and EDXRD: influence of cement type, water-to-cement ratio, and aggregate, Cem. Concr. Res. 36 (2006) 144–159.
[36] R. Tixier, B. Mobasher, Modeling of damage in cement-based materials subjected to external sulphate attack. I: formulation, J. Mater. Civ. Eng. 15 (4) (2003) 305–313.
[37] R.S. Gollop, H.F.W. Taylor, Microstructural and microanalytical studies of sulfate attack III. Sulfate-resisting Portland cement: reactions with sodium and magnesium sulfate solutions, Cem. Concr. Res. 25 (1995) 1581–1590.
[38] R.S. Gollop, H.F.W. Taylor, Microstructural and microanalytical studies of sulfate attack. I. Ordinary portland cement paste, Cem. Concr. Res. 22 (1992) 1027–1038.
[39] P.K. Mehta, In: Concrete, Structure, Properties and Materials, Prentice-Hall, Englewood Cliffs, NJ, 1986, p. 112.
[40] D. Bonen, S.L. Sarkar, Replacement of Portlandite by gypsum in the interfacial zone and cracking related to crystallization pressure, Ceramics Transtractions, vol. 37, Cement-Based Materials Present, Future, and Environmental Aspects American Ceramic Society, Westerville, OH, 1993, 49–59.